

Developing an Inkjet Printer I: RGB Image to CMY Ink Amounts - Image Processing and Color Management*

Yin Wang¹, Baekdu Choi¹, Davi He², Zillion Lin², George Chiu¹, Jan Allebach¹,

¹ Purdue University, West Lafayette, Indiana 47906, U.S.A

² Sunvalleytek International Inc., Shenzhen, CHINA

Abstract

In this paper, we will introduce a novel low-cost, small size, portable nail printer. The usage of this system is to print any desired pattern on a finger nail in just a few minutes. The detailed pre-processing procedures will be described in this paper. These include image processing to find the correct printing zone, and color management to match the patterns' color. In each phase, a novel algorithm will be introduced to refine the result. The paper will state the mathematical principles behind each phase, and show the experimental results, which illustrate the algorithms' capabilities to handle the task.

1. Introduction

Inkjet printing technology has been widely used in the office and in the household. Nowadays, a lot of sizes and brands of inkjet printers that have been designed for different purposes can be found in the market. But the printing medium for those printers is usually a flat surface. This leads to a question: how about using the inkjet technology to print on a small, curved surface, like a finger nail? To be able to print on a finger nail, there are two problems that need to be solved before beginning the printing process: defining the correct printing zone, and applying a color management algorithm to the pattern that is to be printed.

This article will have the following structure. First, Sec. 2 will give an overview of the nail printer product, which includes the system working process and the product's storyboard. In Sec. 3, we will introduce the nail segmentation algorithm. The nail mask acquisition method and the nail edge refinement procedure will be included in this section. Sec. 4 will discuss the color management algorithm and its results. Finally, we will come to the conclusion in Sec. 5.

2. Product Overview

The product we are developing is a small portable printer. This nail printer has size 210 mm × 210 mm × 210 mm, which is a cube. It has a screen built on top of it, which is used as the interface for the customer to choose the desired pattern, and to see the position of their nail inside the printer. Fig. 1 shows an image of the nail printer.

The working process for the whole nail printing system is shown in Fig. 2. There are total of five modules in the whole working process: the nail identification module, the nail curvature module, the halftoning module, the hardware ready bits module, and the printer motor control module. In this paper, we will

be focusing on the nail identification module and the image pre-processing for the halftoning module, which is the color management algorithm. The other modules are described in [1], [2], [3], and [4].



Figure 1: Nail printer overview.

To be able to have a better visualization of the whole working process, a storyboard is provided in Fig. 3 and Fig. 4. We can see from the storyboard that in addition to the nail printer shown in Fig. 1, several gels and a LED light are required. The reason for applying these gels on top of the nail before the whole process is to enable the ink drops to adhere firmly on the nail surface.

3. Nail Segmentation

In this section, we will discuss the nail identification module in Fig. 2. Unlike commonly used inkjet printers that print on media with a standard size, our nail printer will print on a finger nail. As we know, finger nails have various sizes, differing from finger to finger, and person to person. This means that the printing zone in each printing instance is different, and finding the correct printing zone is a critical task in the working process. This is why the nail mask acquisition algorithm is required. After finding the nail mask, we want to refine the nail mask's edge to be able to refine the printing zone. That is to be described in the following section.

Nail Mask Acquisition

Nail mask acquisition includes two main steps. The first step is to capture the image of the finger nail. A gray-scale camera is embedded inside the printer. The real-time finger nail image will be captured; and the finger nail image will be shown on the screen. The resolution of the captured image is 900 × 600 pixels, which is the same as the resolution of the registration box in Fig. 2. In the second step, an algorithm will be applied to the captured image,

*Research supported by Sunvalleytek International Inc, Shenzhen, CHINA.

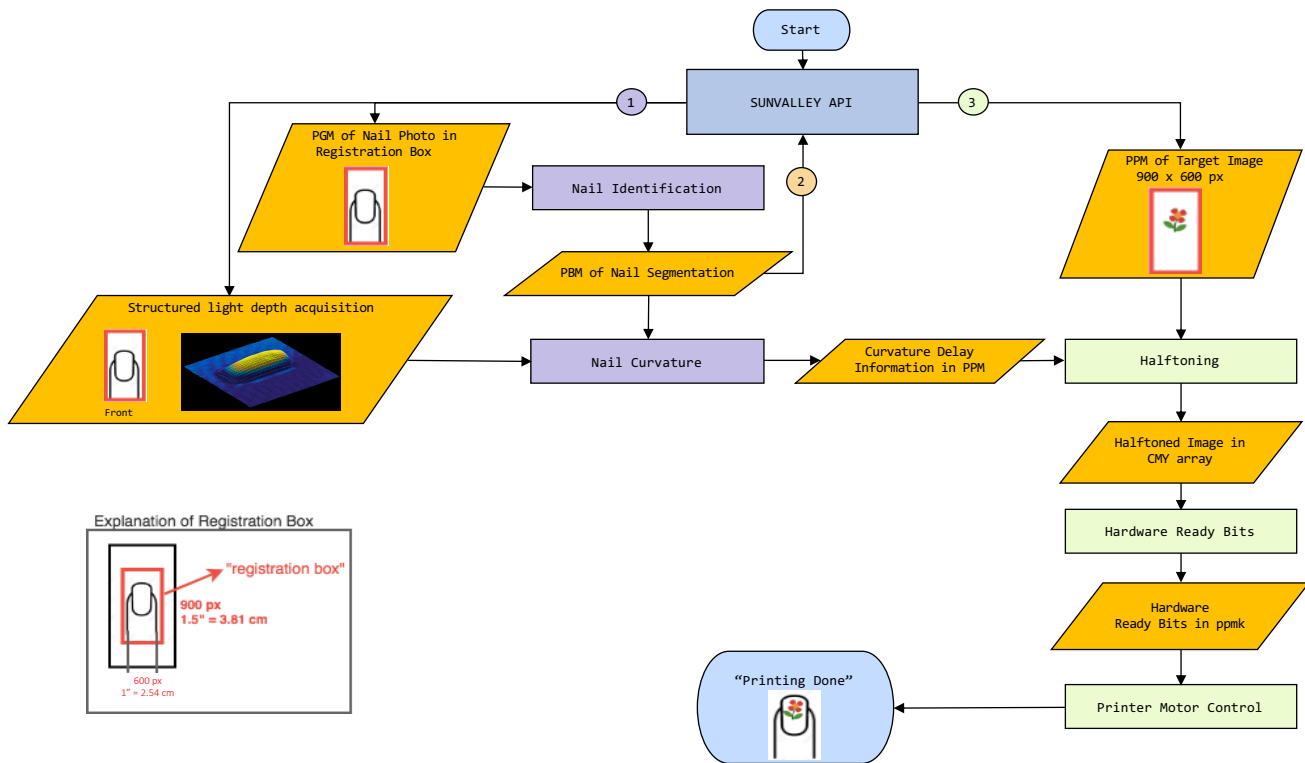


Figure 2: Nail printer working flowchart.

segmenting the nail mask from the background. The segmented nail mask will define the printing zone in the printing process.

The algorithm for segmenting the nail mask can be summarized as follows:

1. Downsample the original gray-scale image by 4 times. Now the image will have a resolution of 225×150 pixels.
2. Rescale the image intensity (gray-level) using the equation:

$$g'[m,n] = \frac{(g[m,n] - \min g[m,n])}{(\max g[m,n] - \min g[m,n])} \times 255 \quad (1)$$

Here $g[m,n]$ represents the pixel graylevel in the down-sampled image, and $g'[m,n]$ is the pixel's graylevel in the rescaled image.

3. Apply Otsu's [5] threshold to binarize the image. Here the background will be classified as black, and the nail mask will be classified as white.
4. Apply a 3×3 erosion [6] to the image.
5. Apply eight neighborhood connected components [7] to the eroded image. The one with the largest area will be kept, and will be regarded as the nail mask area.
6. Check the center point in the image, where the pixel coordinates are (112, 75). If the pixel is white (nail mask), we go forward to the next steps. If the pixel is black (background), we may ask the customer to adjust the finger nail's position, because there is a high possibility that their finger nail is not within the registration box that shown in Fig. 2.
7. Apply a 3×3 image dilation [6] to the image to restore the missing pixels from the image erosion process.

Now we will have a binary image, in which the nail mask is white, and background is black. But there is one more thing that needs

to be considered. If we take a look at the original image (Fig. 6a), we may notice that there is a 'STOP BAR' under the finger nail (Fig. 5a). It has a color that is similar to that of the nail surface. This 'STOP BAR' may exist in the nail mask, as shown in Fig. 5b. So after the last step in nail mask acquisition, we apply a Sobel vertical edge detector, by convolving the nail mask image (Fig.

6b) with the matrix $\begin{bmatrix} 1.5 & 0 & -1.5 \\ 3 & 0 & -3 \\ 1.5 & 0 & -1.5 \end{bmatrix}$, in both the x and y direc-

tions. The resulting image after the convolution and thresholding using Otsu's method [5] can be found in Fig. 5c. Then, if there are vertical lines outside the nail mask area, we count the number of white points in each row. For the rows in which the number of white points is higher than the average number of white points, in each row (from the start row to the end row, as shown in Fig. 5d), we start from the center pixel in each row, and scan from the center pixel to the right side, and stop searching after hitting the first black pixel in this row. All white pixels beyond the first black pixel will be regarded as black. Then we do the same thing from the center pixel to the left side in the same row. All these steps are carried out on the Sobel-filtered and thresholded nail mask shown in Fig. 5c. We then transfer this information to the original nail mask image shown in Fig. 5b to eliminate one row of the 'STOP BAR'. When all the rows between the start row and the end row in Fig. 5d are scanned in this manner, we will have a nail mask without the 'STOP BAR', as shown in Fig. 6b

The original grayscale image can be found in Fig. 6a. And the nail mask after the process described above can be found in Fig. 6b. We can observe that the shape of the nail mask is very similar to the original nail shape, except that the edges are not as smooth as those of the original nail. So we need to do nail edge

refinement, in order to refine the nail mask and the actual printing zone.

Nail Edge Refinement

Now that we have successfully segmented the nail mask from other parts in the image, we want to refine the nail's edge to get a smooth nail mask edge. So an ellipse-shape equation has been purposed to do the task. The equation we have purposed can be expressed as:

$$c(x,y) = |x|^n + |y|^n = 1 \quad (2)$$

where $x \in [0, 1]$, $y \in [0, 1]$, and $n \in (0, \infty)$. The shape of the equation with various values of n is shown in Fig. 7. We can see that when n is small, the line shape is very similar to a straight line, and when n gets extremely big, the shape of the line is like two perpendicular lines. We want to fit the nail edge's curve with different values of n . In the fitting process, we want the nail's four curved corners: upper left, upper right, lower left, and lower right, to be fitted with different values of n , according to their different curvatures. The fitting process can be summarized as follows:

1. In the nail mask image, draw a bounding box around the nail mask (Fig. 8a).
2. On each edge of the bounding box, find two critical points that are the intersection between each side of the bounding box and the nail mask's edge – like the magenta points in Fig. 8b.
3. According to the critical points, segment the nail mask into four quarters as shown in Fig. 8c. In this figure, each segmented quarter is labeled with lines of different colors, and there are overlapping areas between each two quarters. Each quarter is chosen to be as large as possible according to the following procedure: (1). For the upper right quarter, the bottom edge extends to the lowest critical point along the right side of the bounding box; and the left edge extends to the leftmost critical point along the top side of the bounding box. (2). For the upper left quarter, the bottom edge extends to the lowest critical point along the left side of the bounding box; and the right edge extends to the rightmost critical point along the top side of the bounding box. (3). For the lower left quarter, the top edge extends to the highest critical point along the left side of the bounding box; and the right edge extends to the rightmost critical point along the bottom side of the bounding box. (4). Finally, for the lower right quarter, the top edge extends to the highest critical point along the right side of the bounding box; and the left edge extends to the leftmost critical point along the bottom side of the bounding box. According to this procedure, the quarters will generally overlap, as shown in Fig. 8c. These overlapping areas will be processed in a different manner as described in Step 8. Fig. 8d shows an example of one quarter.
4. In the nail mask (Fig. 6b), determine the set of boundary points (x_j, y_j) , $j = 1 \cdots M$ (M is the number of edge points in the nail mask) by using a Sobel operator.
5. In each quarter, for different n values, generate different curves using the equation:

$$\left(\frac{x}{X}\right)^n + \left(\frac{y}{Y}\right)^n = 1 \quad (3)$$

where X and Y are the number of pixels along the x-axis and the y-axis, respectively, in the quarter. Discretize the exponent n in Eq. (3) to $N = 100$ uniformly spaced values, n_i , $i = 1 \cdots N$, ranging from 1 to 10, in steps of size 0.1. For each n_i , compute the total squared distance D between the boundary of the nail profile and the the curve given by Eq. (3). So

$$D = \sum_{j=1}^M \sqrt{(x_j^{mask} - x_j^{curve})^2 + (y_j^{mask} - y_j^{curve})^2} \quad (4)$$

where $(x_j^{curve}, y_j^{curve})$ is the point on the curve that is closest to (x_j^{mask}, y_j^{mask}) , which is identified by determining an expression for the Euclidean distance between the point (x_j^{mask}, y_j^{mask}) and any point that satisfies the Eq. (3). The point $(x_j^{curve}, y_j^{curve})$ that makes the first derivative of the Euclidean distance expression be zero will be the point that we are looking for. And this is the point that will be used in Eq. (4).

6. The value of n that corresponds to the minimum D value will be the final n to be applied in this quarter.
7. Shift the edge points on the mask to the curve points' position, using the selected n value in Step 6. The refinement result for one quarter can be found in Fig. 9.
8. Repeat for all four quarters. For the areas that belong to two quarters, we will calculate the average n values of the quarters to which this area belongs, and take the average n value as the final n that will be used in this area to refine the edge of the nail mask.

The nail edge refinement result is shown in Fig. 6c. We can see that the nail edges are smoother than the mask in Fig. 6b, and the shape is similar to the original nail shape, as shown in Fig. 6a. To visualize the difference between the refined nail mask and the original nail, we overlap the downsampled gray-scale image with the nail mask in Fig. 6c. The result is shown in Fig. 6d. From this image, we can conclude that by using the nail mask acquisition and nail edge refinement methods that are described in this section, we will have a precise printing zone for the working process with the nail printer product.

4. Color Management

The purpose of color management in this project is to match the printed pattern's color appearance to the original digital pattern's color appearance, in order to have a faithful visual reproduction of the pattern printed on a finger nail. Liu et al. [8] has proposed a pipeline of color management for the Indigo press. We followed their ideas to do the gamut mapping, and followed their forward and inverse mapping methods for our nail printer product.

Our color management pipeline is shown in Fig. 10. For a given digital image, we first convert the input color image from the sRGB color space to the YyCx Cz color space, which is a linearized version of the CIE L*a*b* color space. Then, gamut mapping is applied to this image, following the procedures described in [8]. Note that our gamut mapping procedure is image-dependent. So if a given color occurs in two different images, it may be mapped to two different colors depending on the other colors that are present in these two images. Next, we use the inverse table method in order to convert the image from the Yy-CxCz color space to the CMY color space of the printer. Here,

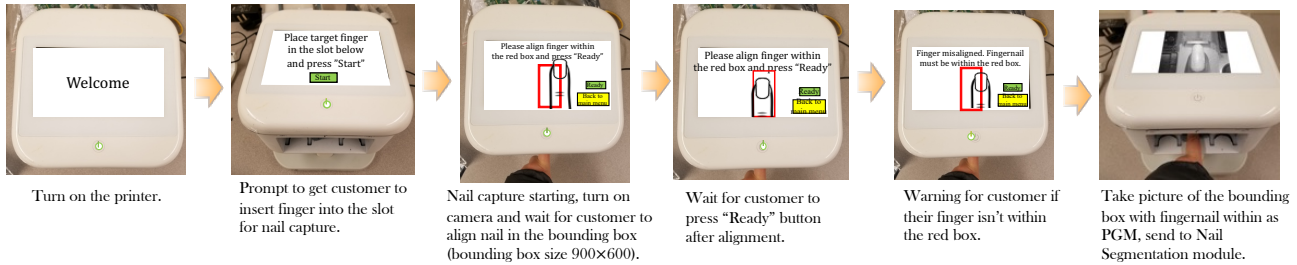


Figure 3: Storyboard (Part 1). Please refer to Fig. 2 for additional information regarding the nail printer working flowchart and the modules that are referenced in this storyboard.

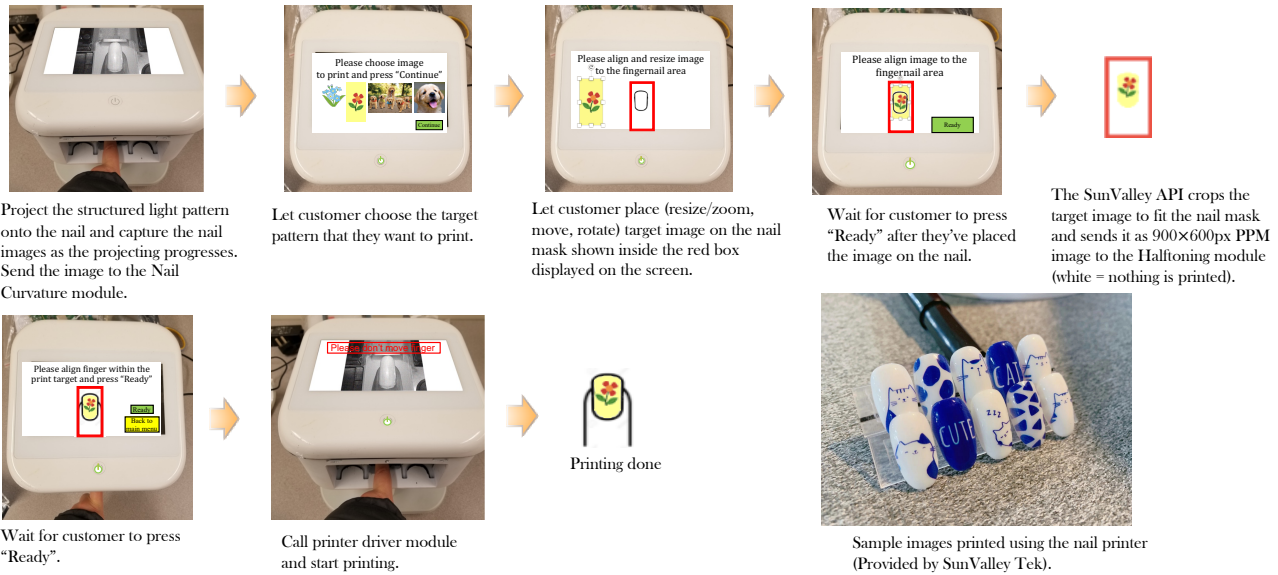


Figure 4: Storyboard (Part 2). Please refer to Fig. 2 for additional information regarding the nail printer working flowchart and the modules that are referenced in this storyboard.

the reason for using a CMY color space is that the nail printer described in this paper only has three colors, which are C (cyan), M (magenta), and Y (yellow). Tone correction to compensate for dot gain follows the inverse table method. Finally, we will have the continuous tone CMY image, which can be delivered to the halftoning module, as shown in Fig. 2.

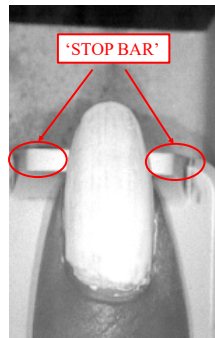
Gamut Mapping

The reason for gamut mapping is that some input colors are not realizable with our nail printer system. To be able to print a pattern with satisfactory visual quality, gamut mapping is needed in the working process. The principles and detailed explanation for our gamut mapping method have been described in [9], [10], [11]. For a given image that is to be printed using the nail printer, we first de-gamma the image, transfer it from sRGB to CIEXYZ, and then from CIEXYZ to YyCx Cz with a D50 white point.

The first step of gamut mapping is to align the neutral axes of the source and printer gamuts. Then, we perform lightness compression for the source gamut, which results in all source gamut points' lightness (Y_y) values being inside the lightness range of the printer gamut. A hue slice to illustrate lightness compression is shown in Fig. 11.

The next step is to perform bounding cylinder compression. In this step, we compress the chroma component $\sqrt{C_x^2 + C_y^2}$ of the source gamut, so that each source gamut point has chroma component not exceeding the maximum chroma component of the printer gamut in the hue slice containing that source gamut point. Fig. 12 shows a hue slice before and after the bounding cylinder compression.

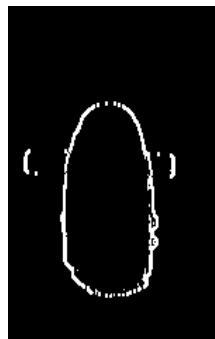
The last step is to do hue slice center compression. Within each hue slice, we compress all the source gamut points toward the hue slice center to bring all source gamut points within that



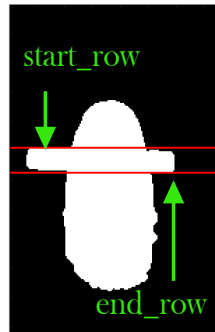
(a) Original gray scale image to illustrate 'STOP BAR'.



(b) Nail mask with 'STOP BAR'.



(c) Nail mask after Sobel vertical edge detector.



(d) Set of rows to be processed for removal of 'STOP BAR', according to the procedure described near the end of the Section Nail Mask Acquisition.

Figure 5: Process for removing the 'STOP BAR' from the nail mask.

hue slice inside the boundary of the gamut in that hue slice. Here, the hue slice center is defined as $(0, Y_{ymid})$, where the coordinates are the chroma value followed by the lightness value, and $Y_{ymid} = \frac{Y_{ywhite,shifted}}{2}$. A hue slice before and after center compression can be found in Fig. 13. After hue slice center compression, the source gamut points are rotated and shifted back in the same way that the printer gamut is rotated and shifted back to its original place.

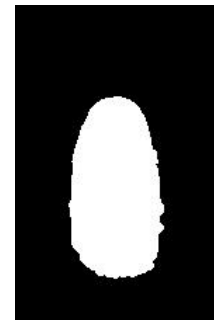
Now, we have done all of the gamut mapping procedure. If we transfer every pixel back to the sRGB space from $YyCx Cz$, the gamut-mapped image can be viewed in Fig. 14a. This result can be compared with Fig. 14b.

Inverse Table Method

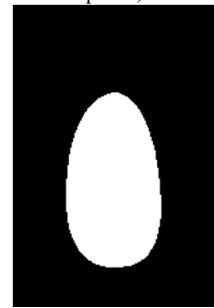
Once the gamut mapping is finished, we need to map to the target CMY value from each pixel's $YyCx Cz$ value. We first generate a table which consists of CMY values for each specific (Yy, Cx, Cz) value. More specifically, we quantize the $YyCx Cz$ color space uniformly so that we can use Yy, Cx, Cz , directly as indices to address values from the inverse table. Then, for each pixel of the gamut mapped image in the $YyCx Cz$ color space, we perform trilinear interpolation to find the corresponding target CMY values using the inverse table.



(a) Original gray scale image from the embedded camera (900×600 pixels).



(b) Nail mask after nail mask acquisition process (225×150 pixels).



(c) Nail mask after edge refinement.



(d) Comparing the nail mask with the gray-scale image.

Figure 6: Original image and nail segmentation result.

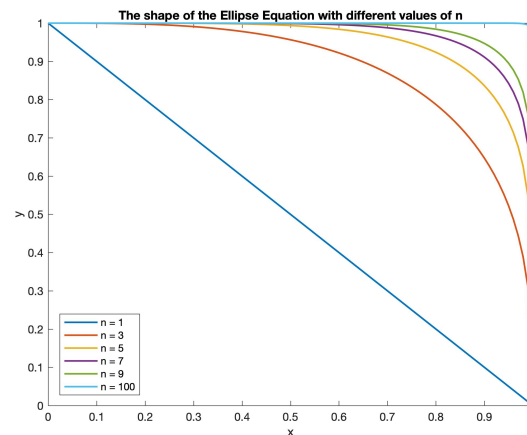


Figure 7: Illustration of the shape of the proposed ellipse-shape equation with different values of n .

5. Conclusion

In this paper, we introduced a novel nail printer, that uses inkjet printing technology to print any desired pattern on a finger nail. The working process and a storyboard for using this nail printer product were described. A novel algorithm to segment and refine the nail mask was introduced to find the correct printing zone as part of the working process. Also, a color management pipeline was described that is used for digital image processing. All these steps result in an image that is ready to print.

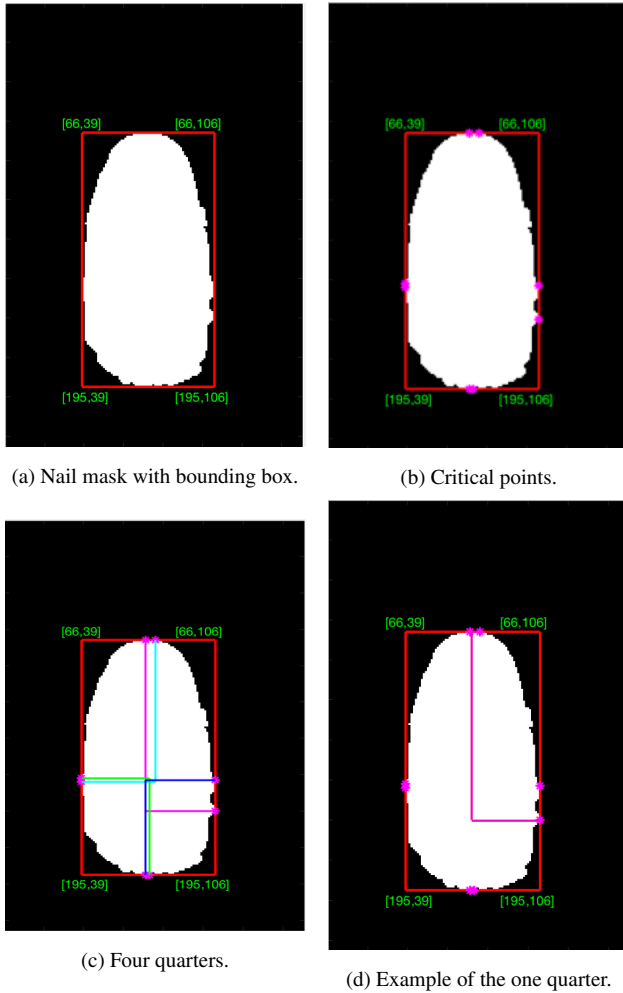


Figure 8: Illustration of nail edge refinement process.

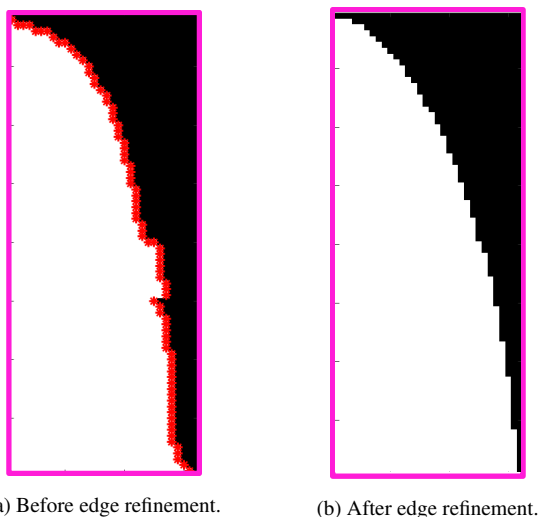


Figure 9: Edge refinement of one quarter.

References

- [1] B. Choi, D. Kenzhebalin, S. Hu, G. Chiu, Z. Lin, D. He, and J. Allebach, "Developing an inkjet printer II: CMY ink amounts to multibit CMY halftones," *Color Imaging XXV: Displaying, Processing, Hardcopy, and Applications*, (Part of IS&T Electronic Imaging 2020), R. Eschbach, G. Marcu, and A. Rizzi, Eds., Burlingame, CA, 26 January - 30 January 2020.

- [2] S. Hu, D. Kenzhebalin, G. Chiu, Z. Lin, D. He, and J. Allebach, "Developing an inkjet printer III: Multibit CMY halftones to hardware-ready bits," *Color Imaging XXV: Displaying, Processing, Hardcopy, and Applications*, (Part of IS&T Electronic Imaging 2020), R. Eschbach, G. Marcu, and A. Rizzi, Eds., Burlingame, CA, 26 January - 30 January 2020.
- [3] D. Kenzhebalin, B. Choi, S. Hu, G. Chiu, Z. Lin, D. He, and J. Allebach, "Developing an inkjet printer IV: Printer mechanism control for best print quality," *Color Imaging XXV: Displaying, Processing, Hardcopy, and Applications*, (Part of IS&T Electronic Imaging 2020), R. Eschbach, G. Marcu, and A. Rizzi, Eds., Burlingame, CA, 26 January - 30 January 2020.
- [4] Y. Wang, Z. Lin, D. He, Z. Lin, B. Robinson, G. Chiu, and J. Allebach, "3D shape estimation for smooth surfaces using grid-like structured light patterns," *Proceedings of 3D Measurement and Data Processing*, (part of Electronic Imaging 2020), W. Puech and R. Sitnik, eds. Burlingame, CA, 26-30 January 2020.
- [5] N. Otsu, "A threshold selection method from gray-level histograms," *IEEE Transactions on Systems, Man, and Cybernetics* 9, no. 1 (1979): 62-66..
- [6] R. Haralick, S. Sternberg, and X. Zhuang, "Image analysis using mathematical morphology," *IEEE Transactions on Pattern Analysis and Machine Intelligence* 4 (1987): 532-550.
- [7] J. Hopcroft, and R. Tarjan. "Algorithm 447: efficient algorithms for graph manipulation." *Communications of the ACM* 16, no. 6 (1973): 372-378.
- [8] J. Liu, T. Frank, Y. Ben-Shoshan, R. Ulichney, and J. Allebach, "NPAC FM Color Halftoning for the Indigo Press: Challenges and Solutions," *Color Imaging XXIV: Displaying, Processing, Hardcopy, and Applications*, (Part of IS&T Electronic Imaging 2019), R. Eschbach, G. Marcu, and A. Rizzi, Eds., Burlingame, CA, 13 January - 17 January 2019.
- [9] W. Xi, T. Frank, Y. Ben-Shoshan, R. Ulichney, and J. Allebach, "Color CLU-DBS Halftoning Based on Neugebauer Primary Area Coverage: Improving the Breed," *Color Imaging XXIII: Displaying, Processing, Hardcopy, and Applications*, (Part of IS&T Electronic Imaging 2018), R. Eschbach, G. Marcu, and A. Rizzi, Eds., San Francisco, CA, 29 January -2 February 2018.
- [10] R. S. Gentile, E. Walowitz, and J. Allebach, "A Comparison of Techniques for Color Gamut Mismatch Compensation," *J. Imaging Technol.*, Vol. 16, pp. 176-181, October 1990.
- [11] M. Wolski, J. Allebach, and C. Bouman. "Gamut mapping squeezing the most out of your color system." *Color and Imaging Conference*, vol. 1994, no. 1, pp. 89-92. Society for Imaging Science and Technology, 1994.

Author Biography

Yin Wang received her B.S. (2016) in Electrical Engineering in Purdue University and currently is a Ph.D. candidate at Purdue ECE. Her research focuses on color image processing, computer vision, 3D reconstruction, and deep learning applications.

Peng (Davi) He (Note: 'He' is his last name) is a software manager in Sunvalleytek International Inc, Shenzhen, Guangdong, China. He received his B.S in Communication Engineering from Hunan University of Arts and Science, Changde, Hunan, China in 2012. His current research interest including artificial intelligence and robot.

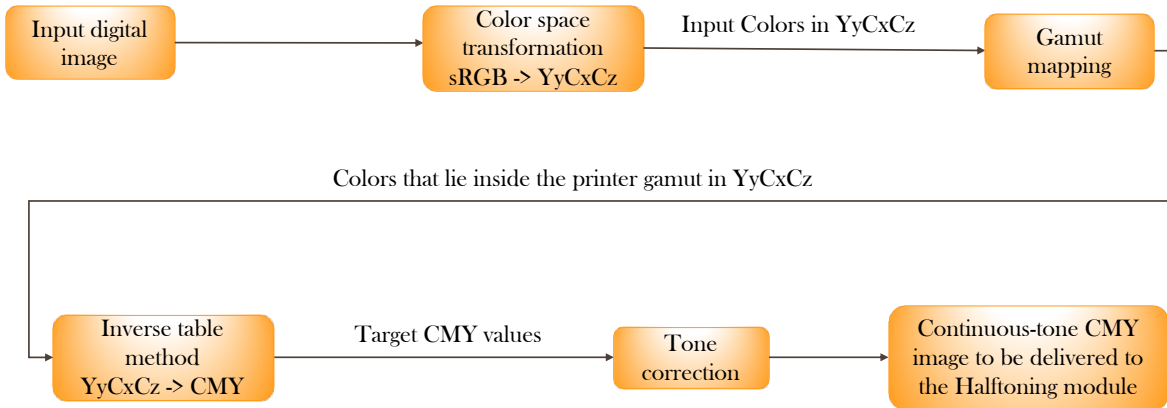
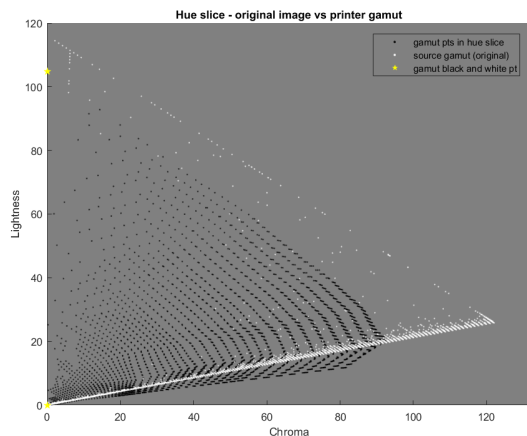
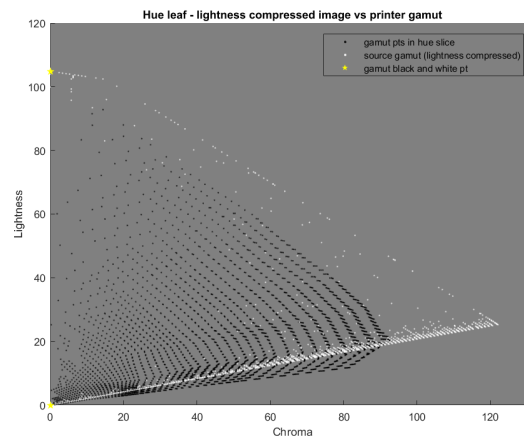


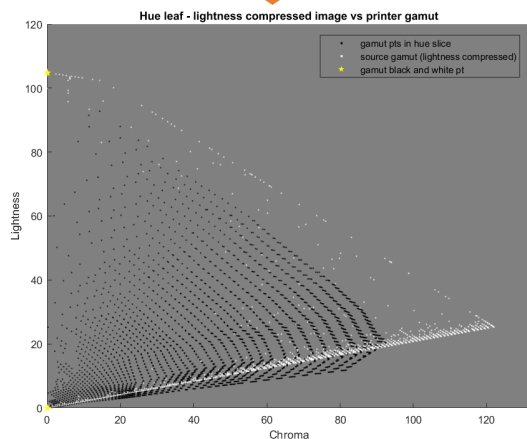
Figure 10: Color management pipeline.



(a). Original image and printer gamut

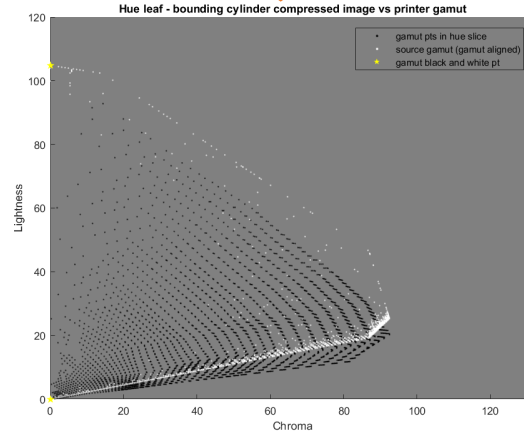


(a). Before bounding cylinder compression



(b). Gamut after lightness compression

Figure 11: Hue slice before and after lightness compression.



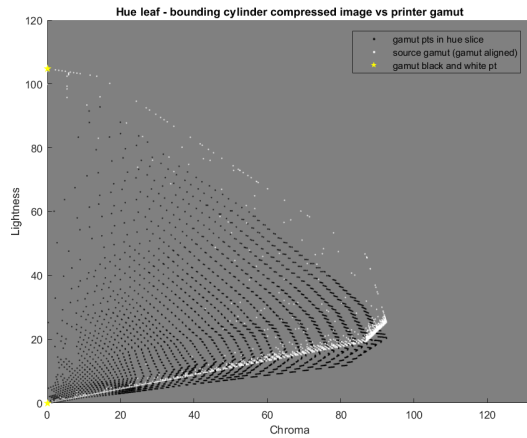
(b). After bounding cylinder compression

Figure 12: Hue slice before and after bounding cylinder compression.

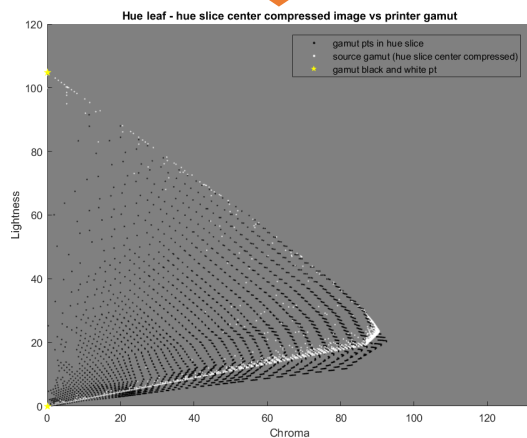
Zillion (Zhenqing) Lin is a technical director in Sumvalleytek International Inc, Shenzhen, Guangdong, China. He received his BS in Microelectronics Engineering from University of Electronic Science and Technology of China, Chengdu, Sichuan, China in 2008 and MS in Biomedical Engineering from Shenzhen University, Shenzhen, Guangdong, China. His current research interest including artificial intelligence and robot.

George T. Chiu is a Professor in the School of Mechanical Engi-

neering with courtesy appointments in the School of Electrical and Computer Engineering and the Department of Psychological Sciences at Purdue University. He also serves as the Assistant Dean for Global Engineering Programs and Partnership for the College of Engineering. Dr. Chiu received the B.S. degree in Mechanical Engineering from the National Taiwan University in 1985 and the M.S. and Ph.D. degrees in Mechanical



(a). Before hue slice center compression



(b). After hue slice center compression

Figure 13: Hue slice before and after hue slice center compression.

Engineering from the University of California at Berkeley, in 1990 and 1994, respectively. From September 2011 to June 2014, he served as the Program Director for the Control Systems Program at the National Science Foundation. His current research interests are mechatronics and dynamic systems and control with applications to digital printing and imaging systems, digital fabrications and functional printing, human motor control, motion and vibration perception and control. He received the 2012 NSF Director's Collaboration Award and the 2010 IEEE Transactions on Control System Technology Outstanding Paper Award. He served as the Editor-in-Chief for the IEEE/ASME Transactions on Mechatronics from 2017-19 and as the Editor for the Journal of Imaging Science and Technology from 2012-14. Dr. Chiu served on the Executive Committee of the ASME Dynamic Systems and Control Division (DSCD) from 2007 to 2014 and as the Chair of the Division from 2012-13. He is a Fellow of ASME and a Fellow of the Society for Imaging Science and Technology (IS&T)

Jan P. Allebach is Hewlett-Packard Distinguished Professor of Electrical and Computer Engineering at Purdue University. Allebach was named Electronic Imaging Scientist of the Year by IS&T and SPIE, and was named Honorary Member of IS&T, the highest award that IS&T bestows. He has received the IEEE Daniel E. Noble Award, the IS&T/OSA Edwin Land Medal, is a Fellow of the National Academy of Inventors, and



(a) Original digital image before gamut mapping.



(b) After gamut mapping.

Figure 14: Digital image before and after gamut mapping.

is a member of the National Academy of Engineering.

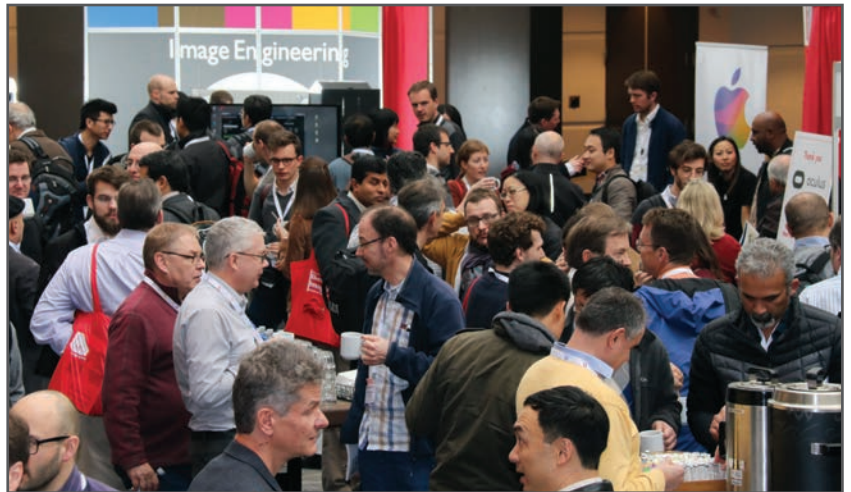
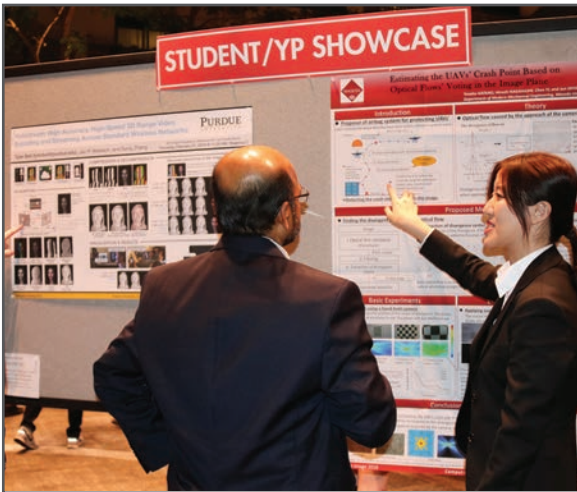
JOIN US AT THE NEXT EI!

IS&T International Symposium on

Electronic Imaging

SCIENCE AND TECHNOLOGY

Imaging across applications . . . Where industry and academia meet!



- **SHORT COURSES • EXHIBITS • DEMONSTRATION SESSION • PLENARY TALKS •**
- **INTERACTIVE PAPER SESSION • SPECIAL EVENTS • TECHNICAL SESSIONS •**

www.electronicimaging.org

